

# **HiSST: 4th International Conference on High-Speed Vehicle Science Technology** 22 -26 September 2025, Tours, France



# Simplified reaction model of n-dodecane combustion for scramjet combustor applications

Youngjin Jun<sup>1</sup>, Seong-kyun Im<sup>2</sup>

#### **Abstract**

The reliable operation of scramjet combustors is hindered by two major challenges: achieving ignition within sub-millisecond residence times and mitigating severe thermal loads on combustor walls. Regenerative cooling with hydrocarbon fuels offers a promising solution, as endothermic thermal cracking simultaneously enhances heat-sink capacity and generates reactive intermediates that promote ignition. Among candidate surrogates, n-dodecane is widely used due to its representative paraffin chemistry and well-characterized thermophysical properties. However, existing detailed mechanisms are too complex for computational fluid dynamics, while no dedicated simplified reaction model for n-dodecane has been available. This study develops a two-step global reaction model for ndodecane-air combustion tailored to scramjet-relevant conditions. The rate parameters are optimized against ignition delay time and laminar flame speed obtained from a reference detailed mechanism. A coarse-to-fine search combined with a sequential filtering framework identified robust parameter sets, ensuring a reasonable accuracy across a broad range of pressure, temperature, and equivalence ratio. Despite the model shows modest deviations under certain conditions, it offers sufficient accuracy for preliminary simulation studies while preserving computational efficiency.

**Keywords**: *n-Dodecane*, *Global reaction*, *Scramjet* 

#### **Nomenclature**

Latin

A – Pre-exponential factor

C – Concentration

E<sub>a</sub> – Activation energy

H – Altitude

K<sub>eq</sub> – Equilibrium constant

Ma – Mach number

P - Pressure

S<sub>L</sub> – Laminar flame speed

T – Temperature

q - Dynamic pressure

n – Concentration exponent

k - reaction rate constant

Greek

Φ – Equivalence ratio

α – Pressure exponent

η – Compression efficiency

σ – Arbitrary combustion characteristics

Page | 1

т – Ignition delay time

ψ – Cycle temperature ratio

 $\omega$  – Net reaction rate

Subscripts

at - Atmospheric

flight - Flight

in - Combustor entry

## 1. Introduction

The development of scramjet propulsion systems is central to the realization of sustained hypersonic

HiSST-2025-138 Copyright © 2025 by author(s)

<sup>&</sup>lt;sup>1</sup> School of Mechanical Engineering, Korea University, 145, Anam-ro, Seongbuk-gu, Seoul 02841, Korea, jyj970522@korea.ac.kr

School of Mechanical Engineering, Korea University, 145, Anam-ro, Seongbuk-gu, Seoul 02841, Korea, sim3@korea.ac.kr

flight. However, scramjet combustors face two critical challenges, namely achieving ignition within extremely short residence times and mitigating severe thermal loads on the combustor walls [1]. At flight speeds above Mach 5, the residence time of gases inside the combustor is typically less than a millisecond, during which fuel injection, mixing, ignition, and flame stabilization must occur [1]. Simultaneously, the intense heat release associated with combustion, compounded by aerodynamic heating, imposes substantial thermal stresses on structural materials [2]. These coupled aerodynamic and chemical constraints define one of the most formidable barriers to reliable scramjet operation.

Regenerative cooling has emerged as a promising strategy to alleviate both ignition and thermal management issues [3]. In this approach, the hydrocarbon fuel is circulated through wall-embedded channels, absorbing heat from the combustor walls. At elevated temperatures, the fuel undergoes endothermic thermal cracking, which not only extends the effective heat-sink capacity but also generates lighter hydrocarbon intermediates with improved ignition characteristics [4]. This dual function makes regenerative cooling particularly attractive for integrated scramjet design.

Among potential surrogate fuels, n-dodecane has gained prominence as a representative of the paraffin class in transportation fuel surrogates [5]. Its thermophysical properties and endothermic cracking behavior have been extensively characterized, providing reproducible datasets for oxidation, pyrolysis, and heat transfer processes [6]. Consequently, n-dodecane has been widely adopted in both experimental and numerical investigations of hydrocarbon combustion and regenerative cooling [4, 7, 8]. However, while detailed chemical kinetic mechanisms for n-dodecane combustion exist and capture low-through high-temperature oxidation pathways, these mechanisms typically involve thousands of reactions and hundreds of species, rendering them computationally intractable for practical computational fluid dynamics (CFD) simulations [5, 9, 10].

Simplified reaction models offer a viable alternative by balancing fidelity with tractability. Previous studies have proposed global reaction models for various hydrocarbons, designed to reproduce laminar flame speeds, ignition delay times, and equilibrium compositions across a range of conditions [11-16]. These simplified models, often comprising one to four global steps, have demonstrated utility in large-eddy simulations and engineering design studies. However, to date no dedicated global reaction model has been proposed for n-dodecane. Moreover, existing efforts often rely on varying rate parameters to match specific targets, whereas CFD practitioners prefer models with fixed Arrhenius parameters that can be easily integrated into reaction flow solvers [13, 16].

The objective of this study is to develop a two-step global reaction model for n-dodecane-air combustion. The model is constructed to simultaneously reproduce ignition delay times and laminar flame speeds over conditions relevant to scramjet combustion, while maintaining the simplicity required for CFD applications. By providing a computationally efficient yet physically representative chemical model, this work aims to enable more reliable and accessible simulations of n-dodecane-fueled scramjet combustors.

### 2. Problem formulation and method

The development of a global reaction for hydrocarbon combustion begins with defining the representative combustor conditions in which the model will be applied. In this work, the entry conditions of a dual-mode scramjet combustor were taken as the target. These conditions were estimated based on flight-representative freestream properties obtained from the U.S. Standard Atmosphere [17]. Static temperature and pressure as functions of altitude is shown in Fig. 1. For supersonic vehicles, the flight envelope is constrained by the dynamic pressure. Excessive value of dynamic pressure leads to intolerable aerodynamic and structural loads, whereas too low values necessitate impractically large lifting surfaces [2]. A representative dynamic pressure of 100 kPa was selected in this work.

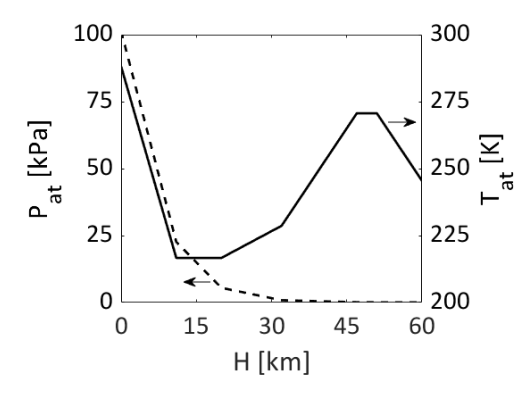
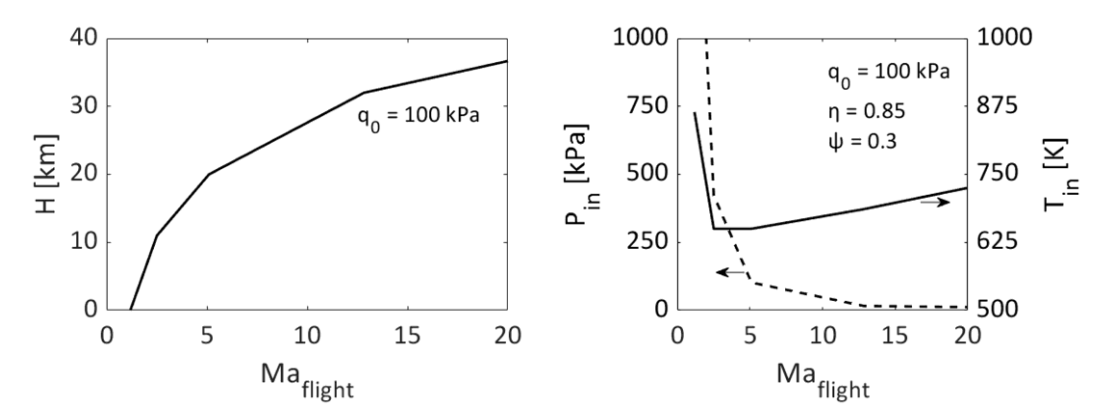


Fig. 1 Variation of static pressure and temperature with altitude.

The burner entry conditions were determined by assuming adiabatic compression of freestream air, a cycle temperature ratio of 3, and a compression efficiency of 0.85. For flight Mach numbers in the range of 5-7 relevant to dual-mode scramjets, the resulting combustor entry conditions are approximately 0.5-1 atm and 600-750 K (Fig. 2), which define the target regime for the model development.



**Fig. 2** Variation of altitude (left) and combustor entry pressure and temperature (right) with flight Mach number along a constant dynamic pressure trajectory.

Hydrocarbon combustion can be represented by different levels of global reaction schemes, ranging from one-step to multi-step. Fig. 3 shows a comparison of adiabatic flame temperature predicted by one-step, two-step, and four-step schemes against reference data. The reference data was obtained from Narayanaswamy's detailed mechanism [5]. The one-step scheme, though computationally efficient, significantly overpredicted flame temperatures in fuel-rich conditions. The four-step scheme achieved high accuracy across the full range of equivalence ratios but at the expense of greater complexity. The two-step scheme was selected as an appropriate compromise, balancing fidelity and computational tractability.

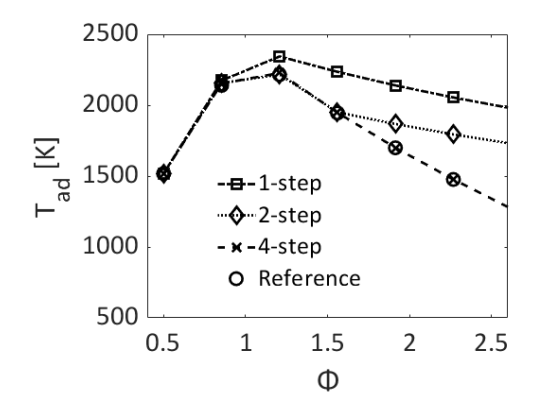


**Fig. 3** Adiabatic flame temperature as a function of equivalence ratio at a fresh gas temperature of 300 K and pressure of 1 atm. Results are compared between the reference mechanism and global reaction schemes with 1, 2, and 4 steps.

HiSST-2025-138 Page | 3 Simplified reaction model of n-dodecane combustion for scramjet combustor applications Copyright © 2025 by author(s) The two-step scheme involves two lumped reactions: (1) the primary oxidation of n-dodecane to CO and H<sub>2</sub>O, and (2) the subsequent oxidation of CO to CO<sub>2</sub>. The chemical equations are shown in Eq. 1 and Eq. 2, respectively. Their respective net rate expressions are:

$$C_{12}H_{26} + 12.5O_2 \rightarrow 12CO + 13H_2O$$
 (1)

$$CO + 0.5O_2 \rightleftarrows CO_2 \tag{2}$$

$$\dot{\omega}_1 = A_1 \cdot exp(-E_{a1}/R_uT) \cdot C_{C_{12}H_{26}}^{n_f} C_{O_2}^{n_0}$$
(3)

$$\dot{\omega}_{1} = A_{1} \cdot exp(-E_{a1}/R_{u}T) \cdot C_{C_{12}H_{26}}^{n_{f}} C_{O_{2}}^{n_{o}}$$

$$\dot{\omega}_{2} = k_{2f} \cdot C_{CO}^{n_{CO}} C_{O_{2}}^{n_{O_{2}}} - \frac{k_{2f}}{K_{eq}} \cdot C_{CO_{2}}^{n_{CO_{2}}}$$

$$\tag{4}$$

The first reaction governs ignition delay and laminar flame speed, while the second ensures correct CO/CO<sub>2</sub> partitioning and adiabatic flame temperature [13]. Rate parameters for the CO oxidation step were adopted from prior studies, whereas those for the primary fuel oxidation were optimized in this work [18].

It is well established that laminar flame speed decreases with increasing pressure. Its dependence on pressure has been represented in previous studies by a correlation of the form [19, 20]:

$$S_L(P) = S_L(P_{ref}) \cdot (P/P_{ref})^{\alpha} \tag{5}$$

Earlier work has shown that the value of  $\alpha$  is approximately related to the effective reaction orders of the fuel and oxidizer [21]:

$$\alpha = (n_f + n_o)/2 \tag{6}$$

Fitting to reference data indicated that the pressure dependence of laminar flame speed is well reproduced with  $\alpha = -0.22$  as illustrated in Fig. 4. Consequently, the reaction orders of the fuel and oxidizer were included as additional adjustable parameters in the optimization procedure. The remaining task was then to determine appropriate values of the pre-exponential factor  $(A_1)$  and activation energy  $(E_{a1})$  of the fuel oxidation reaction that minimize a cost function defined as the deviation between model predictions and reference data:

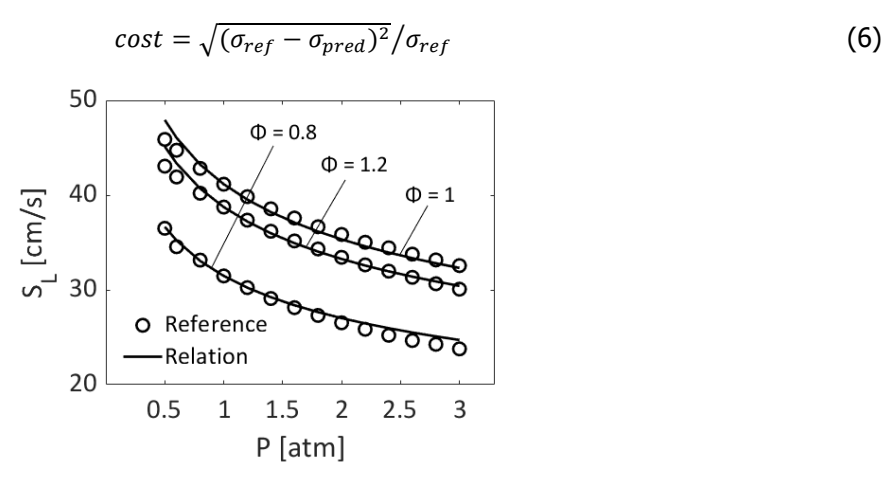
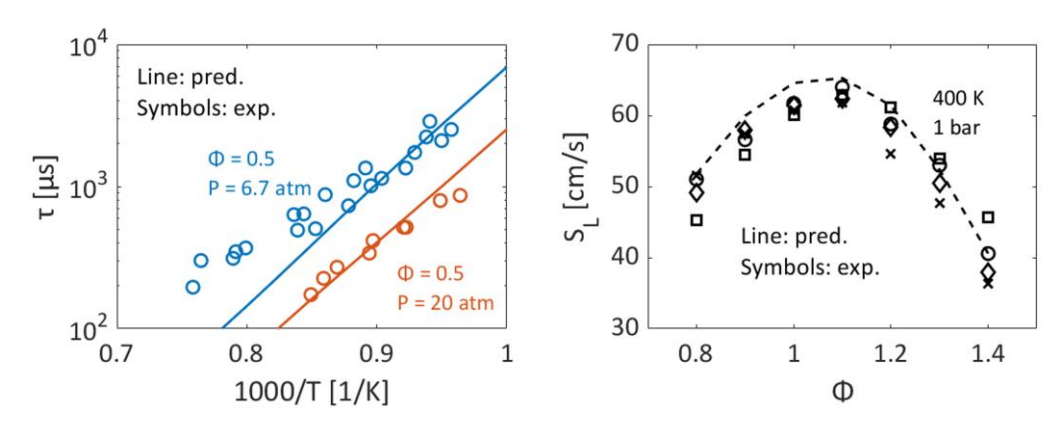


Fig. 4 Variation of flame speed at fresh gas temperature of 300 K with pressure. Results are compared between the reference mechanism and Eq. 5 with  $\alpha = -0.22$ .

The two target combustion characteristics for optimization were ignition delay time and laminar flame speed. Since experimental data is sparse in the relevant thermodynamic range, reference data were drawn from a reference detailed mechanism. Narayanaswamy's detailed mechanism was employed as the reference mechanism, owing to its demonstrated ability to capture both ignition delay time and laminar flame speed across a wide range of conditions [5]. Fig. 5 shows the comparison of ignition delay time and laminar flame speed between the experimental data and the mechanism predictions.



**Fig. 5** Ignition delay time (left) and laminar flame speed (right) compared between experimental data and predictions from the reference mechanism

To search for suitable Arrhenius parameters, a coarse-to-fine algorithm (CTF) was employed. The flowchart of CTF is illustrated in Fig. 6. In this method, the parameter space  $(log(A_1), log(E_{a1}))$  is first sampled on a uniform and coarse grid to identify promising regions. At each stage, all grid points are evaluated and the lowest cost is determined. An adaptive threshold equal to this minimum cost multiplied by a scaling factor, combined with a fixed absolute cap, was used to select candidate points for refinement. Around each selected point, a finer local grid is constructed by halving the step size in both the pre-exponential factor and activation energy directions. This staged refinement concentrated computational effort in the most promising regions of the parameter space while discarding unproductive areas.

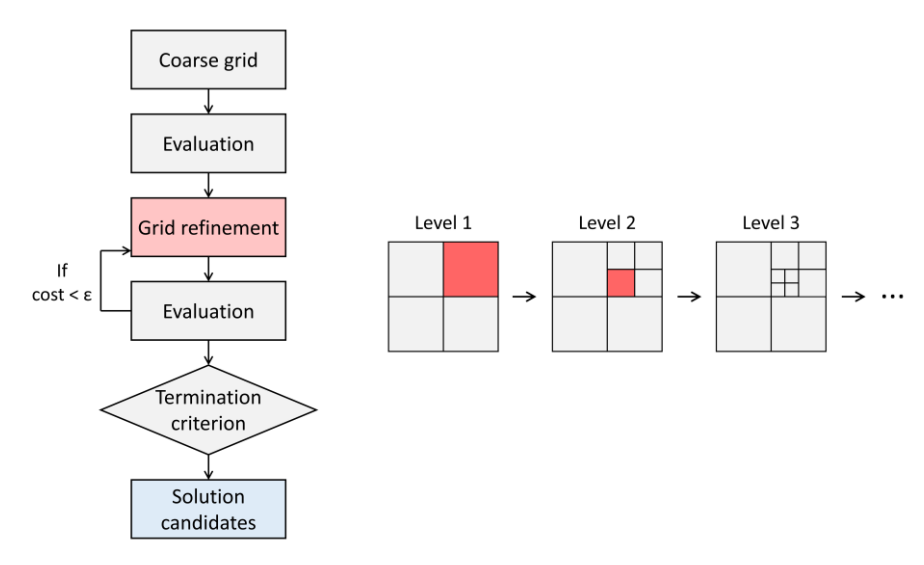


Fig. 6 Schematic procedure of CTF

The resulting pool of candidate solutions from CTF search was then screened using a sequential filtering algorithm (SFA). In this procedure, candidates are first required to meet an absolute error threshold at the baseline condition. Survivors are then tested sequentially at additional conditions. Candidates passing the fixed threshold advance to the next stage. If no candidate satisfied the strict criterion at a given condition, a controlled relaxation was applied: the best error at that stage was identified, and all candidates of cost values within a bounded multiple of this value were retained. Through this sequential screening, only parameter sets demonstrating consistent accuracy across the full range of conditions were preserved.

## 3. Results and discussion

The optimization of the global two-step reaction model began with a coarse-grid search over the solution space. For each selected pair of reaction orders  $(n_f, n_o)$ , the parameter ranges were explored on a 50-by-50 grid spanning  $log(A_1)$  from 5 to 20 and  $log(E_{a_1})$  from 3 to 6. Fig. 7 shows the resulting

HiSST-2025-138 Page | 5 Simplified reaction model of n-dodecane combustion for scramjet combustor applications Copyright © 2025 by author(s) cost values distribution for the representative case  $n_f=0.1$  and  $n_o=1.46$ . To highlight feasible regions, only solutions with costs less than unity are presented. The majority of the search space was populated by infeasible solutions, with the feasible domain confined to a narrow band in the range of  $log(E_{a1})$  from 4 to 5. Contrary to initial expectations, the coarse search suggested that overlapping solutions satisfying both ignition delay time and laminar flame speed criteria might exist.

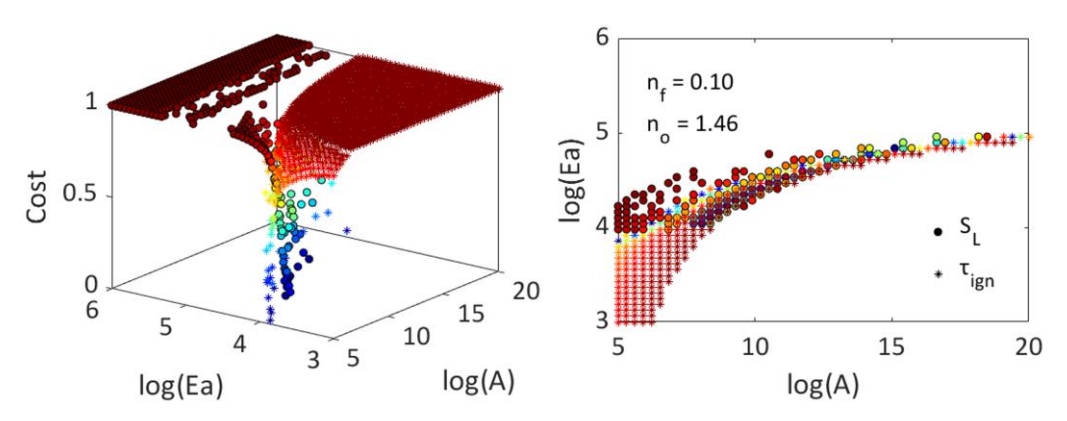


**Fig. 7** Visualization of the cost function over the  $log(A_1) - log(E_{a1})$  space in 3-D (left) and 2-D (right) views.

To progressively narrow the feasible region, successive optimization steps were conducted, refining the intersection between ignition delay time and laminar flame speed solution spaces. The resulting distribution of solution is shown in Fig. 8. These refinements yielded multiple parameter sets that satisfied both ignition delay time and laminar flame speed targets within the optimization window. While several of these candidates performed well at the specific calibration point, further evaluation revealed that their predictive capability does not generalize across the broader condition. This limitation underscored the inadequacy of single-point or locally optimized solutions for CFD applications.

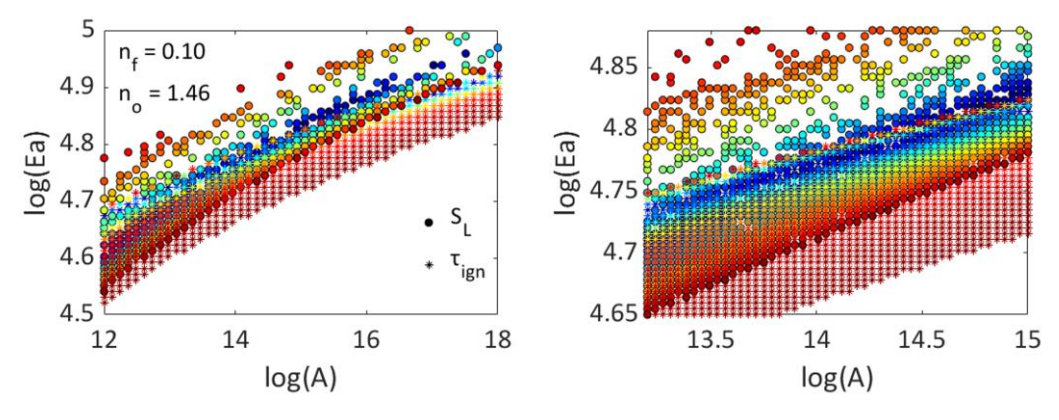


**Fig. 8** Visualization of the cost function over the  $log(A_1) - log(E_{a1})$  space:  $log(A_1)$  from 12 to 18 and  $log(E_{a1})$  from 4.5 to 5.0 (left);  $log(A_1)$  from 13.2 to 15.0 and  $log(E_{a1})$  from 4.65 to 4.88 (right).

Prior to SFA process, a CTF search was performed to generate a diverse population of initial candidate solutions. The underlying rationale is that solutions optimized at isolated conditions may not remain valid at other operating conditions. Hence, a wide pool of candidates is essential for identifying robust parameter sets. Fig. 9 illustrates the evolution of the number of feasible candidate solutions across CTF stages. The number of feasible solutions increased systematically with successive runs. Due to computational constraints, the procedure was terminated after the third stage. By this stage, the search had produced a sufficiently large collection of viable candidates, which then served as the initial seeds for SFA optimization.

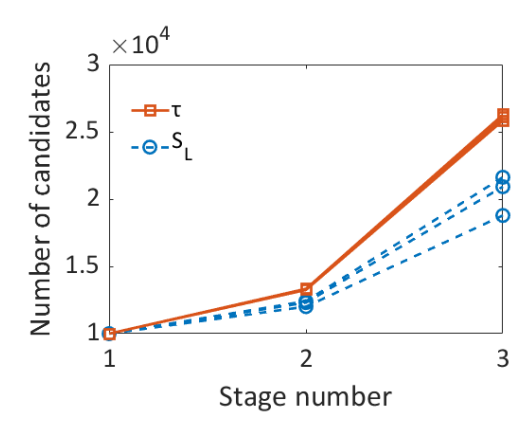
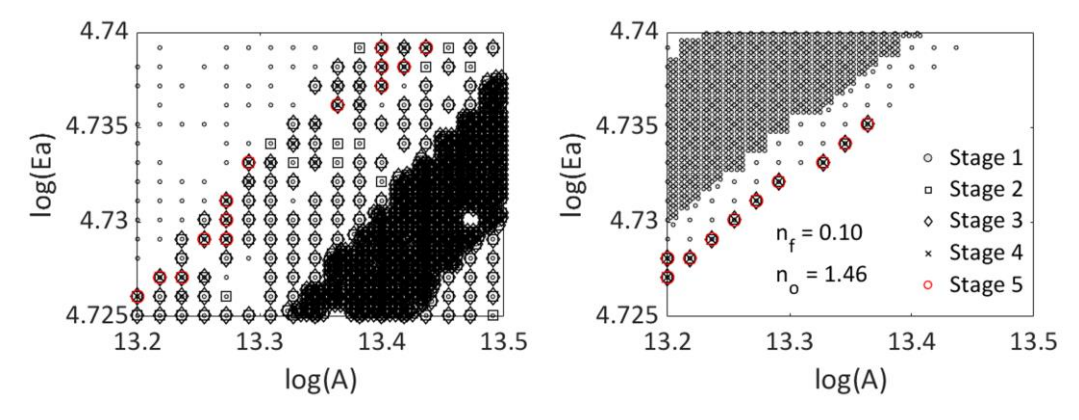


Fig. 9 Number of candidates versus stage number of CTF for ignition delay time and laminar flame speed with  $(n_f, n_o) = (0.1, 1.46), (0.2, 1.36), (0.3, 1.26).$ 

To overcome these shortcomings, a SFA framework was implemented to screen the candidate pool across multiple conditions. The laminar flame speed candidates were evaluated sequentially at equivalence ratios of 1.22, 0.82, 1.5, and 0.67, whereas ignition delay time candidates were evaluated sequentially at fresh gas temperatures of 1125, 1375, 1000, 1500 K. At each stage, candidates passing the fixed threshold were retained. If no candidate met the strict threshold at a given condition, a controlled relaxation was applied. The SFA process ultimately yielded a small set of candidate solutions that are accurate across the prescribed range of conditions as illustrated in Fig. 9. The intersection point between ignition delay time and laminar flame speed feasible solutions was selected as the final optimized set of rate parameters.



**Fig. 10** Distribution of candidate solutions over the  $log(A_1) - log(E_{a1})$  space during SFA optimization. Screening based on laminar flame speed at equivalence ratios of 1, 1.22, 0.82, 1.5, and 0.67 (left), with fresh gas temperature of 300 K and pressure of 1 atm (right). Screening based on ignition delay time at fresh gas temperatures of 1250, 1125, 1375, 1000, and 1500 K with equivalence ratio of 1 and pressure of 1 atm.

Fig. 10 compares the model-predicted ignition delay times with reference data. Overall, the optimized two-step model captures the ignition delay trends across the full range of pressures and temperatures investigated. While the general agreement is strong, modest discrepancies are present. At low pressure (0.5 atm) and elevated temperatures above 1300 K, the model slightly underpredicts ignition delay time. Conversely at higher pressure (3 atm) and lower temperatures below 1100 K, ignition delay time were modestly overpredicted. These deviations, however, are unlikely to significantly impact autoignition of scramjet combustor, where combustor residence times are on the order of millisecond.

HiSST-2025-138 Page | 7 Copyright © 2025 by author(s)

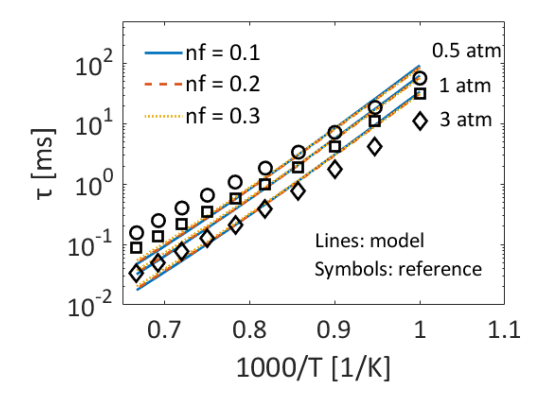


**Fig. 11** Comparison of ignition delay time between predictions from the reference mechanism and the current model at equivalence ratio of 1.

Comparison of laminar flame speed predictions between the model and reference data is shown in the Fig. 11. The model reproduced laminar flame speed trends well across the considered conditions. The best overall agreement was achieved with  $n_f=0.1$ . Discrepancies emerged at equivalence ratios greater than 1.1, where flame speeds were consistently overpredicted. This behavior at fuel-rich conditions is partly attributed to a well-known limitation of the two-step reaction scheme. Despite this limitation, the model demonstrated acceptable accuracy given the broad range of combustion conditions to be covered, and the use of fixed values of rate parameters.

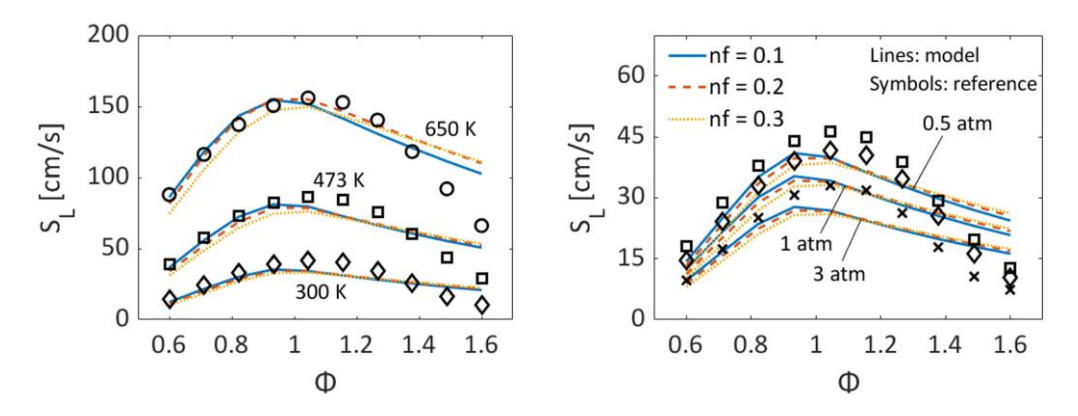


**Fig. 12** Comparison of laminar flame speed between predictions from the reference mechanism and the current model at fresh gas temperature of 300, 473, and 650 K (left), and at pressures of 0.5, 1, and 3 atm (right).

## 4. Conclusion

This study developed a two-step global reaction model for n-dodecane-air combustion for scramjet combustor applications by calibrating rate parameters against ignition delay times and laminar flame speeds. The optimization procedure, including CTF and SFA, yielded a robust parameter set that reproduces reference trends across a broad range of pressure, temperature, and equivalence ratio.

While modest discrepancies remain, particularly at fuel-rich conditions, the model captures the essential combustion characteristics within engineering accuracy. These limitations reflect inherent constraints of a global reaction scheme; nonetheless, the model may offer sufficient accuracy for preliminary design studies, where computational efficiency is a primary concern.

By providing a simplified while preserving essential combustion behavior, this work contributes a useful tool for simulation-driven studies of n-dodecane-fueled scramjets. Future extensions could incorporate more complex multi-step schemes, such as a 4-step scheme, to improve accuracy at fuel-rich conditions. In addition, validation of the model within scramjet combustor simulations will be essential to assess its practical performance. Collectively, these efforts will advance the predictive capability of CFD and support the design of next-generation hypersonic propulsion systems.

#### References

- Journal article
  - 1. Urzay, J.: Supersonic Combustion in Air-Breathing Propulsion Systems for Hypersonic Flight. Annu. Rev. Fluid Mech. 50:593-627 (2018)
  - 2. Heiser, W. H., Pratt, D. T.: Hypersonic Airbreathing Propulsion. American Institute of Aeronautics and Astronautics, Inc. (1994)
  - 3. Kanda, T., Masuva, G., Ono, F., Wakamatsu, Y.: Effect of Film Cooling/Regenerative Cooling on Scramjet Engine Performances. Journal of Propulsion and Power. 10 (1994)
  - 4. Nakaya, S., Tsue, M., Kono, M., Imamura, O., Tomioka, S.: Effects of thermally cracked component of n-dodecane on supersonic combustion behaviors in a scramjet model combustor, Combustion and Flame, 162:3847-3853 (2015)
  - 5. Narayanaswamy, K., Pepiot, P., Pitsch, H.: A chemical mechanism for low to high temperature oxidation of n-dodecane as a component of transportation fuel surrogates. Combustion and Flame. 161:866-884 (2014)
  - 6. Malewicki, T., Brezinsky, K.: Experimental and modeling study on the pyrolysis and oxidation of n-decane and n-dodecane. Proceedings of the Combustion Institute. 34:361-368 (2013)
  - 7. Gascoin, N., Abraham, G., Gillard, P.: Synthetic and jet fuels pyrolysis for cooling and combustion applications. Journal of Analytical and Applied Pyrolysis. 89:294-306 (2010)
  - 8. Zhang, D., Hou, L., Gao, M., Zhang, X.: Experimental and Modeling on Thermal Cracking of n-Dodecane at Supercritical Pressure. Energy & Fuels. 32:12426-12434 (2018)
  - 9. Banerjee, S., Tangko, R., Sheen, D. A., Wang, H., Bowman, C. T.: An experimental and kinetic modeling study of n-dodecane pyrolysis and oxidation. Combustion and Flame. 163:12-30 (2016)
  - 10. Wang, H., Dames, E., Sirjean, B., Sheen, D. A., Tango, R., Violi, A., Lai, J. Y. W., Egolfopoulos, F. N., Davidson, D. F., Hanson, R. K., Bowman, C. T., Law, C. K., Tsang, W., Cernansky, N. P., Miller, D. L., Lindstedt, R. P.: A high-temperature chemical kinetic model of n-alkane (up to n-dodecane), cyclohexane, and methyl-, ethyl-, n-propyl and n-butyl-cyclohexane oxidation hiah temperatures, at JetSurF version https://web.stanford.edu/group/haiwanglab/JetSurF/Index.html (2010).
  - 11. Westbrook, C. K., Dryer, F. L.: Simplified Reaction Mechanisms for the Oxidation of Hydrocarbon Fuels in Flames. Combustion Science and Technology. 27:31-43 (1981)
  - 12. Jones, W. P., Lindstedt, R. P.: Global Reaction Schemes for Hydrocarbon Combustion. Combustion and Flame. 73:233-249 (1988)
  - 13. Franzelli, B., Riber, E., Sanjosé, M., Poinsot, T.: A two-step chemical scheme for keroseneair premixed flames. Combustion and Flame. 157:1364-1373 (2010)
  - 14. Millán-Merino, A., Boivin, P.: A new single-step mechanism for hydrogen combustion. Combustion and Flame. 268:113641 (2024)
  - 15. Hautman, D. J., Dryer, F. L., Schug, K. P., Glassman, I.: A Multiple-step Overall Kinetic Mechanism for the Oxidation of Hydrocarbons. Combustion Science and Technology. 25:219-235 (1981)
  - 16. Cailler, M., Darabiha, N., Veynante, D., Fiorina, B.: Building-up virtual optimized mechanism for flame modeling. Proceedings of the Combustion Institute. 36:1251-1258 (2017)
  - 17. Anonymous: U.S. Standard Atmosphere, 1976. Government Printing Office, Washington DC. (1976)
  - 18. Hakim, L., Lacaze, G., Khalil, M., Sargsyan, K., Najm, H., Oefelein, J.: Probabilistic parameter estimation in a 2-step chemical kinetics model for n-dodecane jet autoignition. Combustion Theory and Modelling. 22:446-466

- 19. Gu, X. J., Haq, M. Z., Lawes, M., Woolley, R.: Laminar burning velocity and Markstein lengths of methane-air mixtures. Combustion and Flame. 121:41-58 (2000)
- 20. Metghalchi, M., Keck, J. C.: Laminar burning velocity of propane-air mixtures at high temperature and pressure. Combustion and Flame. 38:143-154 (1980)
- 21. Poinsot, T., Veynante, D.: Theoretical and Numerical Combustion, second ed. R. T. Edwards (2005)